Biocompatible antimicrobial electrospun nanofibers functionalized with ε-poly-L-lysine

Please, cite as follows:

Georgiana Amariei, Vanja Kokol, Vera Vivod, Karina Boltes, Pedro León, Roberto Rosal, Biocompatible antimicrobial electrospun nanofibers functionalized with ε-poly-L-lysine, International Journal of Pharmaceutics, Volume 553, Issues 1–2, Pages 141-148 2018, ISSN 0378-5173, https://doi.org/10.1016/j.ijpharm.2018.10.037.

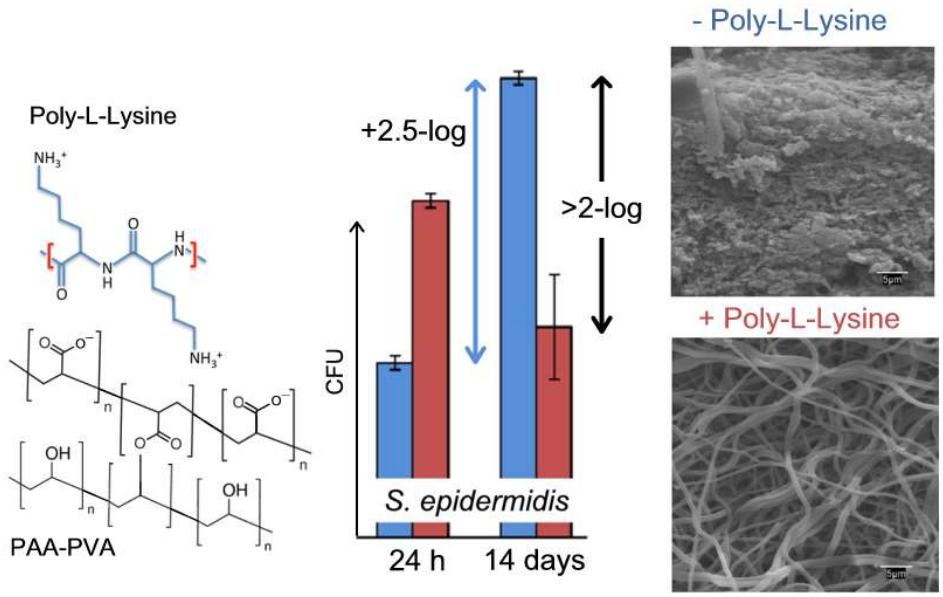

https://www.sciencedirect.com/science/article/pii/S0378517318307725

Biocompatible antimicrobial electrospun nanofibers functionalized with ε-poly-L-lysine

Georgiana Amariei[1], Vanja Kokol[2], Vera Vivod[2], Karina Boltes[1], Pedro Letón[1], Roberto Rosal[1,*]

[1] Department of Chemical Engineering, University of Alcalá, E-28871 Alcalá de Henares, Madrid, Spain
[2] Institute of Engineering Materials and Design, University of Maribor, SI-2000, Maribor, Slovenia
[*] Corresponding author: roberto.rosal@uah.es, Tel.: +34918856395, Fax: +34918855088

Abstract

The antimicrobial polypeptide ε-poly(L-lysine) (ε-PL) was electrostatically incorporated to poly(acrylic acid) (PAA)/poly(vinyl alcohol) (PVA) electrospun nanofibers. ε-PL loading and distribution was assessed by infrared spectra, ζ-potential measurements and the primary amino reactive dye fluorescamine. Functionalized fibers with 485 ± 140 nm diameter, could be loaded with 0.57-0.74 g ε-PL (g dressing)$^{-1}$ that released at a constant rate of 5.4 ± 2.8 mg ε-PL (g dressing day)$^{-1}$. Such a dressings resulted in two orders of magnitude lower bacterial colonization than non-functionalized PAA-PVA after 14 days of incubation. Bacterial impairment was attributed to the damage of cell membranes and the formation of intracellular reactive oxygen species. ε-PL functionalized nanofibers did not display cytotoxicity to human corneal epithelial cells, HCEpC, in 24 h MTT assays. However, the viability of rapidly growing tumoral HeLa cells decreased > 50 % under the same conditions. The prepared biocompatible nanofibrous dressings with durable antibacterial activity show potential application as wound dressings and other biomedical uses.

Keywords: Electrospun fibers; ε-poly(L-lysine); Antibacterial materials; Biocompatible dressings

1. Introduction

Skin injuries represent a significant health challenge. Wound healing is a complex process that requires the transition from an acute inflammatory phase to the successive proliferation and reconstruction phases. Along the process, wound dressings are expected to provide protection against the penetration and proliferation of harmful bacteria and a suitable healing environment for tissue regeneration (Dhivya et al., 2015). Suitable dressing materials should also be capable of maintaining a hydrated environment with proper gas and fluid exchange, among other characteristics, such as non-toxic composition and easiness to apply and remove (Sood et al., 2014). A major requirement is that their biodegradation and biocompatibility profiles support cell growth and proliferation without causing cell toxicity (Dreifke et al., 2015). A number of natural and synthetic materials have been proposed to create dressings meeting different requirements with enhanced functionalities (Parani et al., 2016). Active wound dressings allow the controlled delivery of bioactive agents that include growth factors, enzymes, signaling molecules or antimicrobials (Gainza et al., 2015, Whittam et al., 2016). Antibacterial materials make use of antibiotics, antimicrobial peptides, metal and metal oxide nanoparticles as well as different natural substances including polymeric antimicrobials like chitosan (Felgueiras and Amorim, 2017, Simões et al., 2018).

Antimicrobial peptides are an essential component of innate immunity against pathogenic organisms and have attracted much attention as a novel way of fighting against infections (Epand and Vogel, 1999). ε-Poly-L-lysine (ε-PL) is a cationic homopolyamide naturally produced by the filamentous bacterium *Streptomyces albulus* with a variable number of L-lysine residues, chemically bonded by amide linkage between ε-amino and α-carboxyl groups. It is water-soluble, biodegradable, non-toxic to humans and considered by the US Food and Drug Administration as generally regarded as safe, GRAS, in 2003. ε-PL has a wide antimicrobial capability against bacteria, fungi, yeast, and even molds (Shi et al., 2016, Yoshida and Nagasawa, 2003). Due to these unique characteristics, ε-PL has been proposed for a range of applications, including food preservatives, dietary and emulsifying agents, hydrogels for drug delivery, biodegradable fibers, and biochip coatings (Shi et al., 2016). Poly(L-lysine) polymers loaded in different nanoparticles allow creating biocompatible carriers for drug delivery and gene therapy (Chevalier et al., 2017, Hartono et al., 2012, Zhou et al., 2017). ε-PL has also been used to create tunable tissue engineering materials with antimicrobial functionality (Fürsatz et al., 2018, Hua et al., 2016, Ushimaru et al., 2017).

Hydrogel materials, particularly electrospun fibrous hydrogels, have received considerable interest as dressing materials due to their ability to promote cell migration and proliferation, and to their intrinsic biodegradability (Boateng et al., 2008, Mao et al., 2018). Hydrogels used as polymeric wound dressings include poly(vinyl alcohol)-based membranes,

composites and blends or copolymers with other polymers like poly(acrylic acid) or poly(methyl methacrylate) (Baghaie et al., 2017, Hsieh et al., 2017, Tavakoli et al., 2018). Hydrogels derived from natural polyaminoacids have also be studied for creating wound dressings in view of their good water solubility and biocompatibility (Wang et al., 2016). Recently, the use of poly(acrylic acid) as component of wound dressing formulations has been reported based on its antimicrobial activity, which has been attributed to the binding of carboxylic acid moieties to the divalent cations that stabilize prokaryotic membranes (Amariei et al., 2018, Santiago-Morales et al., 2016). Up to our knowledge, however, ε-PL has not been incorporated into electrospun hydrogel nanofibers. It can be expected that the combinations of ε-PL exceptional features and the versatility of electrospun materials can give rise to novel biomaterials with enhanced application spectrum (Song et al., 2017).

This work aimed at preparing electrospun dressings from ε-PL-functionalized poly(acrylic acid) (PAA) and polyvinyl alcohol (PVA) blends. The material exploits the water solubility of PVA and PAA, the excellent biocompatibility of PVA, and the negative charge of PAA, which is required for the electrostatic adsorption of positively charged peptides. In a previous work, we demonstrated the antimicrobial activity of lysozyme-loaded nanofibers and showed that a small amount of lysozyme retained onto the surface of fibers allowed keeping them free of bacterial proliferation (Amariei et al., 2018). However, lysozyme has two important limitations. First, its low antimicrobial activity in comparison with other peptides. Second, the rapid release observed for adsorbed lysozyme at physiological pH. The rationale of this article was to overcome these limitations by using ε-PL, which is active at much lower concentrations and to establish the biocompatibility of functionalized dressings using cultures of tumoral (HeLa) and epithelial corneal non-tumoral (HCEpC) cells. The antibacterial activity was assessed using the most commonly bacteria found in infected wounds.

2. Materials and methods

2.1. Preparation of electrospun dressings

The polymeric electrospun fibrous scaffold was prepared using the water soluble polymers poly(vinyl alcohol) (PVA, MW 89-98 kDa, 99+% hydrolyzed) and poly(acrylic acid) (PAA, MW 450 kDa), supplied by Sigma-Aldrich (Madrid, Spain). ε-Polylysine or ε-poly-L-lysine (ε-PL, MW 9.1 kDa) was acquired from Zhengzhou Bainafo Bioengineering Co., Ltd. (Henan, China). Fluorescamine was obtained from Sigma-Aldrich (Madrid, Spain). The components of culture media and buffers were purchased from Laboratorios Conda (Spain). Ultrapure water (Millipore Milli-Q System, resistivity > 18 MΩ cm) was used in all experiments.

The PAA-PVA electrospun fibers used as scaffold for the immobilization of AMP were prepared by electrospinning of aqueous solutions containing PAA and PVA as explained elsewhere (Amariei et al., 2018). Briefly, PAA and PVA dissolved in ultrapure water were electrospun with the following operating parameters: working distance 23 cm, flow rate 0.8 mL/h, voltage 23 kV, RH 40%, temperature 25 °C onto a 30 mm diameter drum (PDrC-3000, Yflow Nanotechnology Solutions, Spain) collector rotating at 100rpm. Dry fibers contained 35 wt% PAA (and 65 wt% PVA) were then crosslinked by heating at 140 °C for 30 min, washed, and vacuum dried (10 kPa, 50 °C, 24 h) in order to render insoluble networks. The resulting material was preconditioned in water for 48 h to release non-polymerized material. The scaffold was then dried and used for functionalization. The stability of PAA-PVA crosslinked nanofibers was explained in detail elsewhere (Santiago-Morales et al., 2016).

The immobilization was performed by electrostatic adsorption by immersing PAA-PVA scaffolds in phosphate (pH 7) or carbonate (pH 10) buffer solution containing ε-PL with a molar ratio of 0.5, 1 and 2 with respect to the carboxyl groups of PAA-PVA (7.9 ± 0.3 mmol COOH/g as measured by titration of acid groups). The mixture was kept under constant shaking (100 rpm) for 24 h at room temperature. Then excess ε-PL was removed, the dressings carefully washed and vacuum-dried at room temperature for 24 h. The amount of ε-PL was calculated from total nitrogen content measurements.

2.2. Dressings characterization

Scanning electron microscopy (DSM-950 Zeiss, Oberkochen, Germany) was used to obtain images of dressings that were processed using Image J (National Institute of Health, USA) to determine fiber diameters. Carboxyl content was determined by titration as described elsewhere (Santiago-Morales et al., 2016). Attenuated Total Reflectance Fourier Transform Infrared (ATR-FTIR) spectra were obtained in a Thermo-Scientific Nicolet iS10 apparatus. Non-Purgeable Organic Carbon (NPOC) was determined using a Shimadzu, TOC-VCSH apparatus. Nitrogen content of dressing samples was measured using a LECO CHNS/O-932 elemental analysis equipment. Surface ζ-potential was measured in a Zetasizer Nano-ZS equipment equipped with a surface ζ-potential cell ZEN 1020 (Malvern Instruments Ltd., UK) using PAA (450 kDa) as tracer. Visual observation of ε-PL was accomplished using fluorescamine conjugation as indicated elsewhere (Gao et al., 2014). Labeled peptides were visualized by laser scanning confocal microscope (LSCM, Carl Zeiss LSM5100, Germany), at 365 nm/470 nm excitation/emission wavelengths.

The release of ε-PL from functionalized dressings was studied in phosphate buffered saline (PBS) pH 7.4. Briefly, pieces of samples (about 12.5 mg) were placed into 20 mL bottles with 10 mL medium and incubated at room temperature under mild agitation. The medium was completely replaced with fresh medium at predetermined time intervals. The concentration of ε-PL in solution was quantified by fluorescence using Qubit assay method (Invitrogen) in 96-well microplates. After 30 min of incubation, the fluorescent adduct was determined at 590 nm, upon exciting at 485 nm using a Fluoroskan Ascent FL microplate reader. Each measurement represented the average reading of two adjacent sample wells, and all samples were assayed in triplicate. Under these conditions, ε-PL could be accurately measured in two concentration ranges: low range: 1.56-50 mg/L, and high range: 50-1000 mg/L. The results were presented as cumulative release as a function of time.

2.3. Bioassays

The strains used for antibacterial testing were the gram-positive *S. aureus* (CETC 240) and *S. epidermidis* (CETC 231), and the gram-negative *E. coli* (CECT 516). Minimum inhibition concentrations (MIC, the lowest concentration significantly inhibiting bacterial growth), $EC_{10}$and EC_{50} were determined by measuring colony forming units (CFU) in cultures starting with 10^6 CFU mL^{-1} and incubated at 37 °C for 20 h. Effect concentrations were calculated using a linear interpolation method (Norberg-King, 1993). Agar diffusion tests were performed by placing dressings onto the surface of agar plates inoculated with 10^6 CFU mL^{-1} bacterial suspension and incubated for 14 days at 37 °C. Liquid incubation tests were carried out placing accurately weighed samples into the wells of sterile 6-well plates and incubated in the same way. To determine the number of cells attached to dressing surface, colonized specimens were first washed in PBS for 15 min at 5 °C under orbital shaking in order to remove non-adhered cells. The cells attached to the surface were then recovered with SCDLP broth (Soybean casein digest broth with lecithin and polyoxyethylene sorbitan monooleate) and plate counted. The antibiofilm efficiency was studied using CLSM. Bacterial viability was tracked using Live/Dead BacLight viability kit (Thermo Fisher Scientific). Oxidative stress was measured using 2',7'-dichlorodihydrofluorescein diacetate, which is sensitive for hydrogen peroxide and other ROS, including hydroxyl and peroxyl radicals. For SEM images, samples were double washed with PBS, fixed in glutaraldehyde, dehydrated with gradient ethanol and acetone and dried before gold sputter coating.

The *in vitro* cytotoxicity of the nanofibrous dressings was investigated using the 3-(4,5 dimethylthiazol-2-yl)-2,5-diphenyltetrazolium bromide (MTT) assay with tumoral (HeLa) and human corneal epithelial cells (HCEpC). Prior to the assay, non-functionalized dressings were autoclaved at 121 °C for 30 min and subsequently loaded with sterilized ε-PL solution obtained by filtration through 200-nm syringe filters. The functionalized materials were dried at room temperature under sterile conditions. For the MTT assay, cells were seeded in 24-well plates at a density of 1.5-2 x 10^4 cells per well and allowed to attach to plates for 72 h. Then, cells were incubated with ε-PL loaded dressings (∼5 mg) for 24 h using non-loaded dressings as controls. Wells without nanofibers were used as control. After incubation nanofibers were removed and the remaining cells treated with MTT (5 mg mL^{-1} in PBS) for 4 h at 37 °C. Subsequently, 150 µL dimethylsulfoxide (DMSO) was added per well to dissolve the formazan produced by reduction of the tetrazolium dye. The absorbance was recorded at 570 and 630 nm and cell viability obtained from the amount of formazan generated by the activity of dehydrogenases, which is proportional to the number of living cells.

2.4. Statistical analysis

A one-way ANOVA coupled with Tukey's HSD (honestly significant difference) post-hoc test was performed for comparison of means. Statistically significant differences were considered to exist when p-value < 0.05.

3. Results and Discussion

3.1. Characterization of functionalized electrospun nanofibers

PAA-PVA were stabilized by crosslinking esterification and water immersion until constant weight. The stability of fibers was confirmed by assessing that the amount of non-crosslinked materials was < 0.5 mg NPOC/g membrane (equivalent to < 0.05 wt%) after 48h. The fibers used in this work were water preconditioned for 48 h. FTIR spectra and SEM micrographs of stabilized fibers are shown in Figs 1 and 2 respectively.

The amount of ε-PL immobilized on functionalized dressings is shown in Table 1 together with the surface charge measured at pH 7. Significant immobilization took place for ε-PL, reaching values in the 0.57-0.74 g ε-PL (g dressing)$^{-1}$ range that can be explained in terms the electrostatic self-assembly between the negatively charged PAA-PVA material (ζ-potential -36.5 ± 1.2 mV) and the positive charges of ε-PL (Choi et al., 2015). ε-PL is a homo-polyamide of 25–35 L-lysine residues, bonded together through amide linkage between ε-amino and α-carboxyl groups, which is with isoelectric point 10.5 and, therefore, positively charged at neutral pH (Kaisersberger-Vincek et al., 2016). The electrostatic self-assembly mechanism is consistent with the lower amount of ε-PL immobilized at pH 10, close to the isoelectric point of the polypeptide

(Hyldgaard et al., 2014, Jiang et al., 2010). Non-electrostatic adsorption cannot be totally excluded as polar interactions have been shown to play a role in the interaction of peptides and hydrogels (Zustiak et al., 2013).

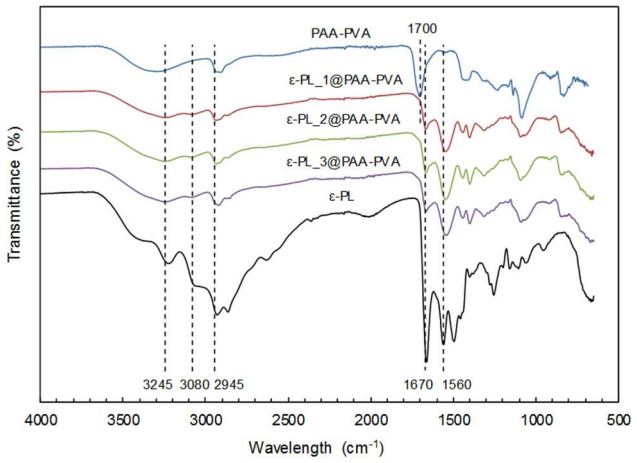

Figure 1. ATR-FTIR spectra of PAA-PVA nanofibers, ε-PL, and ε-PL-loaded dressings (functionalized at pH 7).

The amount of ε-PL immobilized on functionalized dressings is shown in Table 1 together with the surface charge measured at pH 7. Significant immobilization took place for ε-PL, reaching values in the 0.57-0.74 g ε-PL (g dressing)$^{-1}$ range that can be explained in terms the electrostatic self-assembly between the negatively charged PAA-PVA material (ζ-potential -36.5 ± 1.2 mV) and the positive charges of ε-PL (Choi et al., 2015). ε-PL is a homo-polyamide of 25–35 L-lysine residues, bonded together through amide linkage between ε-amino and α-carboxyl groups, which is with isoelectric point 10.5 and, therefore, positively charged at neutral pH (Kaisersberger-Vincek et al., 2016). The electrostatic self-assembly mechanism is consistent with the lower amount of ε-PL immobilized at pH 10, close to the isoelectric point of the polypeptide (Hyldgaard et al., 2014, Jiang et al., 2010). Non-electrostatic adsorption cannot be totally excluded as polar interactions have been shown to play a role in the interaction of peptides and hydrogels (Zustiak et al., 2013).

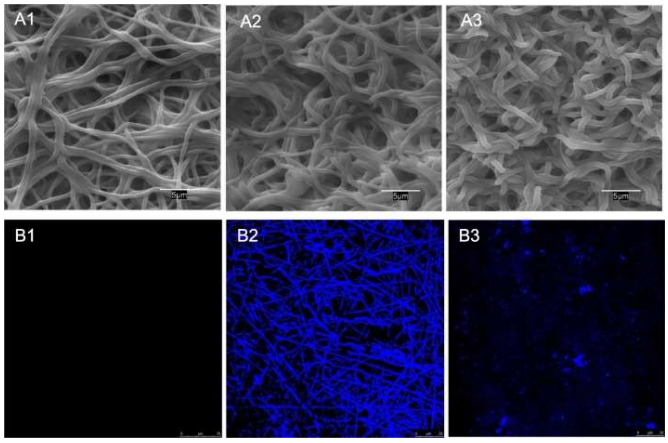

Figure 2. SEM images (A) and confocal laser scanning microscopy images (B) of fibers before impregnation (A1/B1), and after impregnation (ε-PL_1@PAA-PVA) impregnated at pH 7 (A2/B2) and pH 10 (A3/B3). Confocal laser scanning microscopy images of fluorescamine-conjugated fibers revealed ε-PL in blue.

The amount of ε-PL in fibers increased with the concentration of loading solution in a non-linear way suggesting surface saturation. A previous work demonstrated the adsorption of the antimicrobial peptide lysozyme on PAA-PVA nanofibers. Significantly, the amount of ε-PL loaded was about five times lower than that of lysozyme under similar conditions (Amariei et al., 2018). The difference could be attributed to the different conformation of ε-PL and lysozyme. While the latter is a globular protein, ε-PL exhibits a more linear random-coil conformation at pH below its isoelectric point offering poorer interaction with fiber surface (Fukushima et al., 1994, Lu et al., 1999). The lower amount of ε-PL also results in more negatively charged fibers, with surface ζ-potentials in the -15.4-(-22.6) mV range. The large excess of carboxyl groups made surface charge negative in all cases. This result is relevant as negatively charged surfaces are expected to repel bacterial adhesion as a result of the electrostatic interaction with the negatively charged bacterial surface (Rzhepishevska et al., 2013).

Figs. 1 and S1 (Supplementary Material, SM) show the ATR-FTIR spectra of dressings. The FTIR spectra of unloaded PAA-PVA displayed the bands associated

Table 1. The quantity and ζ-potential of differently ε-PL-functionalized dressings. (Dressings denoted as 1, 2 and 3 used of 0.5, 1 and 2 mol ε-PL/mol COOH in PAA-PVA non-functionalized material).

	g ε-PL (g dressing)$^{-1}$		Surface ζ-potential (mV)*	
Nanofibers	pH 7	pH 10	pH 7	pH 10
ε-PL_1@PAA-PVA	0.57 ± 0.24	0.030 ± 0.001	-22.6 ± 1.0	-30.6 ± 3.2
ε-PL_2@PAA-PVA	0.70 ± 0.02	0.034 ± 0.002	-16.7 ± 0.1	-29.2 ± 2.6
ε-PL_3@PAA-PVA	0.74 ± 0.16	0.071 ± 0.036	-15.4 ± 0.2	-25.5 ± 2.6

* Measured at pH 7. The surface ζ-potential of non-functionalized PAA-PVA fibers was -36.5 ± 1.2 mV.

with the polymeric components PAA and PVA. The broad O–H stretching band (3200-3600 cm^{-1}), the C–H alkyl stretching band (2850–3000 cm^{-1}), and the C-O stretching at 1142 cm^{-1} are characteristic features of PVA, while the carboxyl stretching frequency of PAAappeared at 1700 cm^{-1}(Amariei et al., 2017). ε-PL-loaded specimens showed the characteristic absorption bands at 1670 cm^{-1} and 1560 cm^{-1} were attributed to the stretching vibration band of C=O in amide groups, and the bending variation of -NH groups, respectively (Liang et al., 2014). These two amide absorption bands confirmed the existence of amide groups and correspond to the random coil conformation adopted by ε-PL at low pH (Chiou et al., 1992). The absorptions at 3245 cm^{-1} and 3080 cm^{-1} were attributed to the Fermi resonance generated from the frequency multiplication of the amide absorption band II and the stretching vibration of -NH, respectively. The peaks at 3430 cm^{-1} and 2945 cm^{-1} were attributed to the asymmetric stretching of -NH_2 group and the stretching of C-H bonds, respectively.

The SEM micrographs of Fig. 2 (A) show the morphology of nanofibrous dressings. All materials preserved their fibrous structure after impregnation with little difference between functionalized and non-functionalized fibers. The diameter of individual functionalized fibers was (485 ± 140 nm, 50 measurements) with occasional merging between adjacent fibers. A full set of SEM images is included in Fig. S2 (SM). Fig. 2 (B) shows CLSM images of dressings stained with the amine-reactive dye fluorescamine. Fluorescence was absent in non-functionalized fibers but clearly observed in ε-PL loaded materials. Homogeneous distribution took place for impregnation at pH 7, while lower fluorescence readings were recorded at pH 10 consistent with the results shown in Table 1. Fig. S3 (SM) shows CLSM images of all dressings. The pattern of aggregates that appeared for fibers impregnated at pH 10 is consistent with the α-helix structure of ε-PL near its isoelectric point. The FTIR signature of α-helix can be distinguished from the amide-I band at 1650 cm^{-1} in Fig. S1. At pH < 9, however, ε-PL is highly charged and homogeneously adsorbs on PAA-PVA.

3.2. Antibacterial activity

The antimicrobial activity of ε-PL was assessed by determining the inhibitory effect of different doses on the capacity of forming bacterial colonies. MIC, EC_{10} (a surrogate of no-effect concentration) and EC_{50} values are shown in Table 2. The full dose-response curve is shown in Fig. S4 (SM). MIC, EC_{10} and EC_{50} values showed the similar sensitivity to ε-PL, with lower MIC, EC_{10} and EC_{50} values for *S. epidermidis*. MIC values of 3.1 and 12.5 mg $L^{-1}$for *E. coli* and *S. aureus* respectively were reported for ε-PL (25-35 mer) (Hamano et al., 2014). For the same 25-35 mer MIC values against *E. coli* strains were in the 2-4 mg L^{-1}range (Shi et al., 2016). MIC values, about 30 mg L^{-1} were observed for 7 kDa (55 mer) ε-PL against *E. coli* and *S. aureus* strains, which compare well with those reported here for 9.1 kDa (70 mer) (Dai et al., 2015). The antibacterial mechanism of ε-PL against gram-positive and gram-negative bacteria has been attributed to membrane disruption (Fürsatz et al., 2018, Ye et al., 2013). Moreover, the antimicrobial activity of ε-PL has been shown to be closely related to the number or repetitive L-lysine residues (Hyldgaard et al., 2014). Once internalized, ε-PL induced the generation of reactive oxygen species, alteration on various gene expressions and repair mechanisms, and, eventually cell apoptosis and death (Ye et al., 2013). The generation of ROS was significant for the concentration indicated as MIC-ROS in Table 2, which is similar to CFU-based MIC in agreement with the expected role of oxidative stress in ε-PL toxicity mechanism.

Table 2. Dose-effect parameters for bacterial growth inhibition (EC_x are given with their 95% confidence intervals and MIC with the experimental intervals indicating the lower and higher assayed concentrations; concentrations in mg L^{-1}.)

mg L^{-1}	*S. aureus*	*S. epidermidis*	*E. coli*
MIC	0.78 (0.39-1.56)	0.20 (0.10-0.39)	3.13 (1.56-6.25)
EC_{10}	0.28 ± 0.09	0.15 ± 0.08	1.71 ± 0.25
EC_{50}	8.5 ± 1.2	2.4 ± 0.3	15.0 ± 0.6
MIC-ROS	1.56 (0.78-3.13)	0.20 (0.10-0.39)	3.13 (1.56-6.25)

The antibacterial activity of ε-PL functionalized nanofibers in agar diffusion tests only resulted in clear halo zones for *S. epidermidis* (Fig. 3). Images for the three microorganisms incubated with all tested membranes is given in Figs. S5 to S7 (SM). Certain antimicrobial activity was observed for the non-functionalized PAA-PVA material that decreased along the 14-day experiments. In dressings loaded with ε-PL, however, the effect increased with incubation time. The inhibition halo observed after 14 d clearly indicated that the antimicrobial activity was retained for time periods of clinical relevance. The lack of observable halo zones for *E. coli* and *S. aureus* cultures was probably a consequence of the higher concentrations of ε-PL required to inhibit *E. coli* and *S. aureus* growth (Table 2). Assuming that the maximum amount of ε-PL loaded in functionalized dressings got evenly dispersed into the agar plates, the concentration of ε-PL would be < 0.15 mg/L, lower than their MIC, which explain the absence of inhibition halo in their cultures.

The formulation ε-PL_1@PAA-PVA, pH 7, was selected for quantitative CFU measurements. Colony numbers are shown in Fig. 4 for the liquid culture in contact with dressings (A, B and C) and for the bacteria detached from surface (D). All ε-PL-loaded fibers

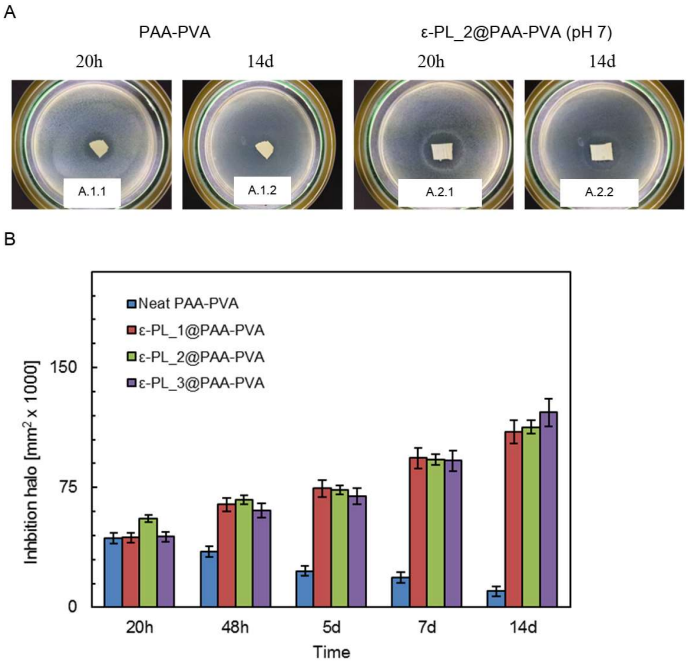

Figure 3. Representative images of inhibition experiments corresponding to non-functionalized PAA-PAA (A.1.1/2), and ε-PL_2@PAA-PVA at pH 7 (A.2.1/2). Halo inhibition zone expressed in mm^2 along 14 day experiments with cultures of *S. epidermidis* in agar plates at 37 °C (B).

displayed higher CFU inhibition than non-functionalized dressings. It was previously reported that PAA-containing polymers display antimicrobial activity due to the chelation of divalent cations of bacteria by carboxylic acid moieties (Gratzl et al., 2015, Santiago-Morales et al., 2016). The antimicrobial effect of PAA-containing fibers was also clearly observed in this work with CFU in liquid cultures displaying up to 1-log inhibition for *S. epidermidis* after 14 days (Fig. 4 B). The effect was higher to the gram-positive bacteria (Fig. 4 A and B) than to the gram-negative *E. coli* (Fig. 4 C) due to their different cell wall structures. Gram-positive are prone to suffer destabilization upon quelation of the divalent cations that stabilize their peptidoglycan envelope, which in gram-negative bacteria is protected by an outer membrane (Clifton et al., 2015, Domingues et al., 2014). Fig. 4 shows significant differences between functionalized and non-functionalized dressings after 72 h. The antimicrobial activity of PAA-PVA would be responsible for the short-term effect observed for non-loaded dressings, but after 48 h, the release of ε-PL maintained significantly lower CFU counts with differences increasing with time.

The antimicrobial effect of ε-PL-functionalized dressings can be clearly observed by comparing CFU in the extracts detached from dressing surface after 24 h and 14 days of exposure (Fig. 4 D). While non-functionalized PAA-PVA was unable to avoid surface colonization with surface CFU in the order of 10^7 CFU mg^{-1}, ε-PL-loaded dressings were significantly less colonized after 14 days in contact with bacterial cultures. All materials displayed viable cell counts below 10^5 CFU mg^{-1}, 2-log less than PAA-PVA under

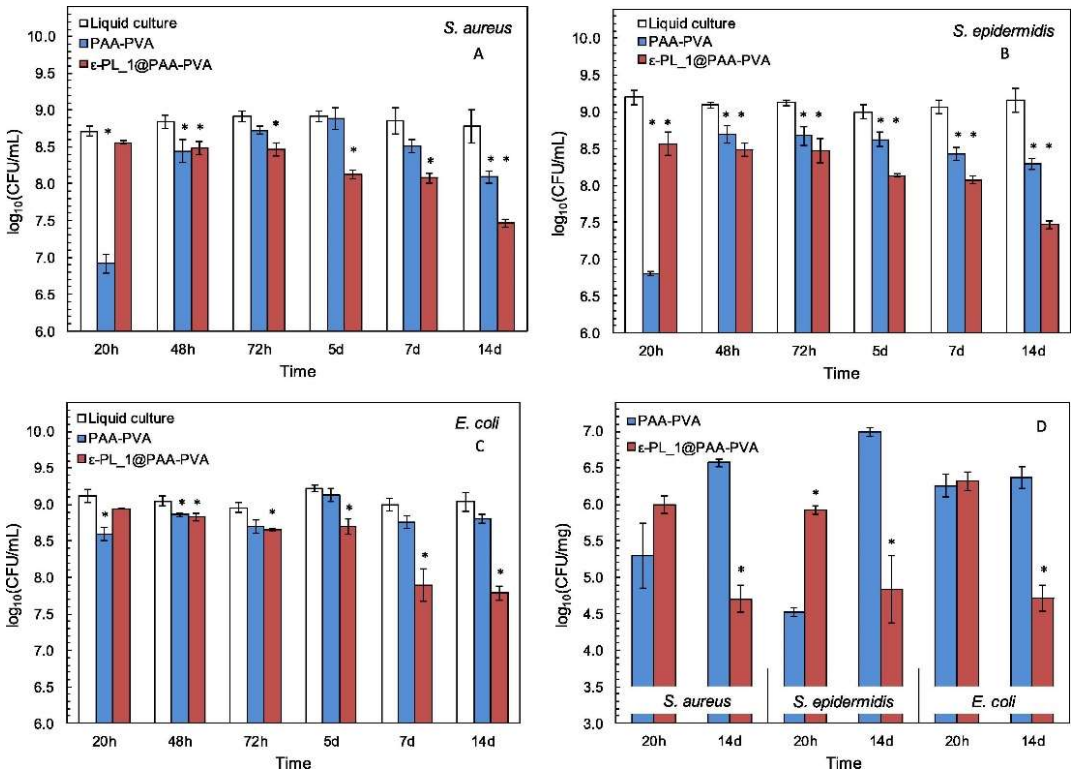

Figure 4. Colony-forming units (CFU) in liquid media in contact with non-functionalized dressings (PAA-PVA) and ε-PL_1@PAA-PVA dressings prepared at pH 7: *S. aureus* (A), *S. epidermidis* (B) and *E. coli*(C), as well as CFU/mg for microorganisms detached from membranes. The white bars of Figs. A, B and C correspond to control cultures without any dressings. Significand differences are marked with asterisks.

the same conditions. The antibiofilm effect against the three strains was apparent from SEM images of dressings exposed to bacterial colonization. The images are shown in Fig. 5 in which the dressing surface of non-functionalized PAA-PVA appeared clearly colonizing by bacterial biofilms. On the contrary, ε-PL-loaded dressings were essentially free of bacteria, with scattered bacterial cells and absence or extracellular biofilm structure.

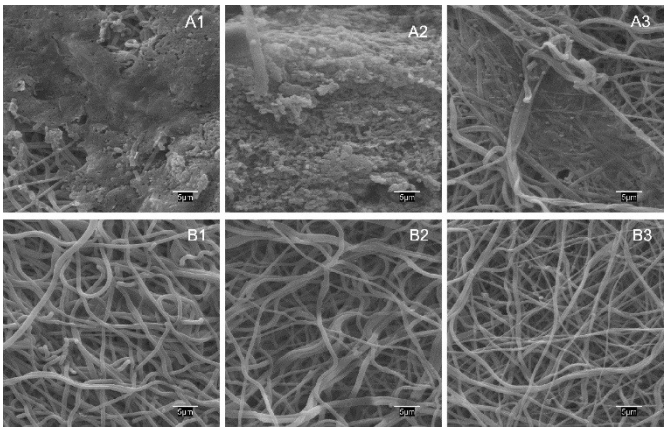

Figure 5. SEM micrographs of non-functionalized PAA-PVA (A) and ε-PL_1@PAA-PVA dressings prepared at ph7 (B) after 14 days in contact with S. aureus (A1, B1), S. epidermidis (A2, B2) and E. coli (A3, B3) at 37 °C.

The anti-fouling capacity and the cell damage were also revealed by the confocal Live/Dead images in Fig S8 (SM). Using the Live/Dead staining, SYTO9 green-labelled cells corresponded to non-damaged bacteria, while PI revealed as red-marked membrane-damaged bacteria. Non-functionalized PAA-PVA dressings were covered by a considerable amount of viable green-labelled bacterial cells after 14 days (Fig. S8 A1-C1). However, Live/Dead confocal images of loaded PAA-PVA dressings under the same conditions showed extensive cell impairment with essentially all cells becoming red-stained for all bacterial strains (Fig.S8 A2-C2). Red-marked cells were those internalizing PI and damaged in cell membrane integrity showing that the antibacterial activity was linked to membrane disruption.

The release profiles of ε-PL (Fig. S9, SM), help to explain the observed results. The experiments showed that the amount of ε-PL released during the first 2 h was ~10 %, and was still slightly below 50% after 14 days. After the first 24 h, the release was practically linear with a sustained rate of 5.4 ± 2.8 mg ε-PL (g dressing day)$^{-1}$. Fig. S9 also shows the ATR-FTIR spectra of dressings freshly prepared and after 14 days in PBS. The spectrum of used dressings still showed the characteristic peaks of ε-PL demonstrating that the nanofibres were capable of retaining it after two weeks. Adsorbed ε-PL is required to preserve the antibiofouling capacity of functionalized dressings and explain the bacterial counts below 10^5 CFU mg^{-1} observed in exposed dressings. In a previous work, we studied the functionalization of the same base material with the antimicrobial peptide lysozyme, but in that case, lysozyme released rapidly at physiological pH and, therefore the dressing displayed lower long-term antimicrobial capacity than ε-PL-loaded fibers (Amariei et al., 2018). Another advantage of ε-PL is that the enzymatic mode of action of lysozyme is evaded by many bacterial strains that produce modified muramidase resistant peptidoglycan as a natural evolutive protection (Masschalck and Michiels, 2003).

3.3. *In vitro* cell proliferation bioassays

The cytocompatibility of materials is essential for their use as wound dressings. MTT *in vitro* viability assays were performed for ε-PL-loaded dressings in HeLa human cervix epithelioid carcinoma and human corneal epithelial cells (HCEpC) in order to explore the biocompatibility of ε-PL loaded nanofibers as well as their differential effects on the viability of rapidly growing cancer cells compared to non-tumoral cells. The results after 24 h are shown in Fig. 6 in which viability refers to controls cells incubated in the absence of dressing.

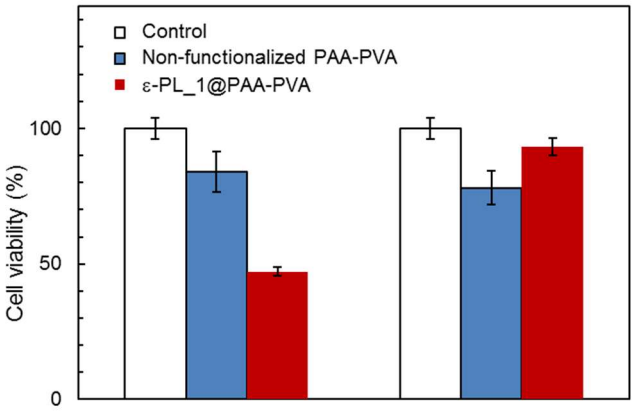

Figure 6. Cytotoxicity of ε-PL_1@PAA-PVA dressing prepared at pH 7 against tumoral HeLa cells (left) and non-tumoral corneal epithelial HCEpC cells (right). Significant differences marked as asterisks.

Non-functionalized PAA-PVA nanofibers impair HeLa and HCEpC cells viability -17 % and -22 % respectively. However functionalized nanofibers were cytotoxic for HeLa cells with 53 % viability inhibition, whereas for non-tumoral HCEpC cells, growth was not significantly affected after 24 h of incubation. The results indicated that ε-PL loaded nanofibres did not induce viability impairment against normal non-tumoral epithelial HCEpC cells. Poly(L-lysine) homopolymers are used as carriers for drug and gene delivery (Shi et al., 2015). The cytotoxicity of polycationic substances is important for biomedical applications and can be modulated by proper molecular weight selection and by regulating the rate of release from composite materials (Hartono et al., 2012). Generally, the toxicity of

cationic polymers is related to the interaction of the primary amine surface groups with cell membrane. Accordingly, it was found that plasma membrane damage and mitochondrially mediated apoptosis were most prominent upon exposure of high molecular weight rather than low molecular weight poly(L-lysine) (Symonds et al., 2005). ε-PL and its composites have been associated to cytotoxicity to cancer cell lines in mitochondrial membrane disruption and the induction of apoptotic pathways via caspase-mediated apoptotic pathways were observed (Paul et al., 2014). ε-PL-loaded polymeric microparticles based on poly(lactic acid) displayed important antiproliferative effect against human pancreatic adenocarcinoma cell lines at concentrations in the 25-100 mgL^{-1} range (Chevalier et al., 2017). Our results showed that the relatively low cytotoxicity of ε-PL-based materials turns into antitumoral effect for the rapidly dividing HeLa cells. This result is in agreement with the low cytotoxicity of ε-PL-loaded materials (Fürsatz et al., 2018). The good biocompatibility and antimicrobial activity observed in this work indicated that ε-PL loaded dressings are candidates as wound dressings and other biomedical applications.

4. Conclusions

We designed and prepared dressings incorporating ε-PL on PAA-PVA electrospun nanofibers. The adsorption was driven by electrostatic self-assembly and allowed loading 0.57-0.74 g ε-PL (g of dressing)$^{-1}$. After the first 24 h, the antimicrobial peptide released from functionalized dressings at a rate of 5.4 ± 2.8 mg ε-PL (g dressing day)$^{-1}$ in PBS at pH 7.4 and ∼50 % was still retained after two weeks.

The antibacterial effect of ε-PL was higher to *S. epidermidis* (MIC 0.20 mg L^{-1}, EC_{50} 2.4 ± 0.3 mg L^{-1}) with MIC, EC_{10} and EC_{50} in the order *S. epidermidis* > *S. aureus* > *E. coli.* The impairment suffered by bacteria could be associated to the damage of cell membranes and the formation of intracellular oxidative species.

The differences in antibacterial efficiency between ε-PL-functionalized and non-functionalized fibers reached one order of magnitude after 14 days for liquid cultures in contact with growing cultures. ε-PL-loaded dressings were considerably less colonized after 2 weeks, displaying viable bacterial counts below 10^5 CFU mg^{-1}, about 2-log less than non-functionalized PAA-PVA.

ε-PL-loaded dressings showed excellent biocompatibility to human corneal epithelial cells (HCEpC), the viability of which was not significantly affected after 24 h. However, tumoral HeLa cells were considerably impaired, with viability losses over 50 %. Overall, our study provides a new insight to prepare biocompatible nanofibrous dressings with durable antibacterial and antifouling efficiency, and potential application as wound dressings or other medical uses.

Acknowledgements

Financial support for this work was provided by the Spanish Ministry of Economy and Competitiveness, CTM2016-74927-C2-1-R and the Dirección General de Universidades e Investigación de la Comunidad de Madrid, Research Network S2013/MAE-2716. GA thanks the University of Alcalá for the award of a pre-doctoral grant.

References

Amariei, G., Kokol, V., Boltes, K., Letón, P., Rosal, R., 2018. Incorporation of antimicrobial peptides on electrospun nanofibres for biomedical applications. RSC Advances 8, 28013-28023.

Amariei, G., Santiago-Morales, J., Boltes, K., Leton, P., Iriepa, I., Moraleda, I., Fernandez-Alba, A.R., Rosal, R., 2017. Dendrimer-functionalized electrospun nanofibres as dual-action water treatment membranes. Science of the Total Environment 601-602, 732-740.

Baghaie, S., Khorasani, M.T., Zarrabi, A., Moshtaghian, J., 2017. Wound healing properties of PVA/starch/chitosan hydrogel membranes with nano Zinc oxide as antibacterial wound dressing material. Journal of Biomaterials Science, Polymer Edition 28, 2220-2241.

Boateng, J.S., Matthews, K.H., Stevens, H.N.E., Eccleston, G.M., 2008. Wound healing dressings and drug delivery systems: A review. Journal of Pharmaceutical Sciences 97, 2892-2923.

Clifton, L.A., Skoda, M.W.A., Le Brun, A.P., Ciesielski, F., Kuzmenko, I., Holt, S.A., Lakey, J.H., 2015. Effect of divalent cation removal on the structure of gram-negative bacterial outer membrane models. Langmuir 31, 404-412.

Chevalier, M.T., García, M.C., Gonzalez, D., Gomes-Filho, S.M., Bassères, D.S., Farina, H., Alvarez, V.A., 2017. Preparation, characterization and in vitro evaluation of □-polylysine-loaded polymer blend microparticles for potential pancreatic cancer therapy. Journal of Microencapsulation 34, 582-591.

Chiou, J.S., Tatara, T., Sawamura, S., Kaminoh, Y., Kamaya, H., Shibata, A., Ueda, I., 1992. The α-helix to β-sheet transition in poly(l-lysine): Effects of anesthetics and high pressure. Biochimica et Biophysica Acta (BBA) - Protein Structure and Molecular Enzymology 1119, 211-217.

Choi, J.H., Kim, S.O., Linardy, E., Dreaden, E.C., Zhdanov, V.P., Hammond, P.T., Cho, N.J., 2015. Influence of pH and surface chemistry on poly(L-lysine) adsorption onto solid supports investigated by quartz crystal microbalance with dissipation monitoring. Journal of Physical Chemistry B 119, 10554-10565.

Dai, X., An, J., Wang, Y., Wu, Z., Zhao, Y., Guo, Q., Zhang, X., Li, C., 2015. Antibacterial amphiphiles based on ε-polylysine: synthesis, mechanism of action, and cytotoxicity. RSC Advances 5, 69325-69333.

Dhivya, S., Padma, V.V., Santhini, E., 2015. Wound dressings – A review. BioMedicine 5, 22.

Domingues, M.M., Silva, P.M., Franquelim, H.G., Carvalho, F.A., Castanho, M.A.R.B., Santos, N.C., 2014. Antimicrobial protein rBPI21-induced surface changes on Gram-negative and Gram-positive bacteria.

Nanomedicine: Nanotechnology, Biology and Medicine 10, 543-551.
Dreifke, M.B., Jayasuriya, A.A., Jayasuriya, A.C., 2015. Current wound healing procedures and potential care. Materials Science and Engineering: C 48, 651-662.
Epand, R.M., Vogel, H.J., 1999. Diversity of antimicrobial peptides and their mechanisms of action. Biochimica et Biophysica Acta (BBA) - Biomembranes 1462, 11-28.
Felgueiras, H.P., Amorim, M.T.P., 2017. Functionalization of electrospun polymeric wound dressings with antimicrobial peptides. Colloids and Surfaces B: Biointerfaces 156, 133-148.
Fukushima, K., Sakamoto, T., Tsuji, J., Kondo, K., Shimozawa, R., 1994. The transition of α-helix to β-structure of poly(d-lysine) induced by phosphatidic acid vesicles and its kinetics at alkaline pH. Biochimica et Biophysica Acta (BBA) - Biomembranes 1191, 133-140.
Fürsatz, M., Skog, M., Sivlér, P., Palm, E., Aronsson, C., Skallberg, A., Greczynski, G., Khalaf, H., Bengtsson, T., Aili, D., 2018. Functionalization of bacterial cellulose wound dressings with the antimicrobial peptide □-poly-L-Lysine. Biomedical Materials 13, 025014.
Gainza, G., Villullas, S., Pedraz, J.L., Hernandez, R.M., Igartua, M., 2015. Advances in drug delivery systems (DDSs) to release growth factors for wound healing and skin regeneration. Nanomedicine: Nanotechnology, Biology and Medicine 11, 1551-1573.
Gao, C., Yan, T., Du, J., He, F., Luo, H., Wan, Y., 2014. Introduction of broad spectrum antibacterial properties to bacterial cellulose nanofibers via immobilising ε-polylysine nanocoatings. Food Hydrocolloids 36, 204-211.
Gratzl, G., Walkner, S., Hild, S., Hassel, A.W., Weber, H.K., Paulik, C., 2015. Mechanistic approaches on the antibacterial activity of poly(acrylic acid) copolymers. Colloids and Surfaces B: Biointerfaces 126, 98-105.
Hamano, Y., Kito, N., Kita, A., Imokawa, Y., Yamanaka, K., Maruyama, C., Katano, H., 2014. □-Poly-L-lysine peptide chain length regulated by the linkers connecting the transmembrane domains of □-poly-L-lysine synthetase. Applied Environmental Microbiology 80, 4993-5000.
Hartono, S.B., Gu, W., Kleitz, F., Liu, J., He, L., Middelberg, A.P.J., Yu, C., Lu, G.Q., Qiao, S.Z., 2012. Poly-l-lysine functionalized large pore cubic mesostructured silica nanoparticles as biocompatible carriers for gene delivery. ACS Nano 6, 2104-2117.
Hsieh, H.T., Chang, H.M., Lin, W.J., Hsu, Y.T., Mai, F.D., 2017. Poly-methyl methacrylate/polyvinyl alcohol copolymer agents applied on diabetic wound dressing. Scientific Reports 7, 9531.
Hua, J., Li, Z., Xia, W., Yang, N., Gong, J., Zhang, J., Qiao, C., 2016. Preparation and properties of EDC/NHS mediated crosslinking poly (gamma-glutamic acid)/epsilon-polylysine hydrogels. Materials Science and Engineering: C 61, 879-892.
Hyldgaard, M., Mygind, T., Vad, B.S., Stenvang, M., Otzen, D.E., Meyer, R.L., 2014. The antimicrobial mechanism of action of □-poly-L-lysine. Applied Environmental Microbiology 80, 7758-7770.
Jiang, M., Popa, I., Maroni, P., Borkovec, M., 2010. Adsorption of poly(l-lysine) on silica probed by optical reflectometry. Colloids and Surfaces A: Physicochemical and Engineering Aspects 360, 20-25.
Kaisersberger-Vincek, M., Štrancar, J., Kokol, V., 2016. Antibacterial activity of chemically versus enzymatic functionalized wool with ε-poly-L-lysine. Textile Research Journal 87, 1604-1619.
Liang, C., Yuan, F., Liu, F., Wang, Y., Gao, Y., 2014. Structure and antimicrobial mechanism of varepsilon-polylysine-chitosan conjugates through Maillard reaction. International Journal of Biological Macromolecules 70, 427-434.
Lu, J.R., Su, T.J., Howlin, B.J., 1999. The effect of solution pH on the structural conformation of lysozyme layers adsorbed on the surface of water. The Journal of Physical Chemistry B 103, 5903-5909.
Mao, X., Sun, X., Cheng, L., Cheng, R., Zhang, Y., Cui, W., 2018. 13 - Hydrogel fibrous scaffolds for accelerated wound healing, in: Guarino, V., Ambrosio, L. (Eds.), Electrofluidodynamic Technologies (EFDTs) for Biomaterials and Medical Devices. Woodhead Publishing, pp. 251-274.
Masschalck, B., Michiels, C.W., 2003. Antimicrobial oroperties of lysozyme in relation to foodborne vegetative bacteria. Critical Reviews in Microbiology 29, 191-214.
Norberg-King, T.J., 1993. A linear interpolation method for sublethal toxicity: The inhibition concentration (ICp) approach (version 2.0), in: US Environmental Protection Agency, N.E.T.A.C., Environmental Research Laboratory-Duluth (Ed.), Duluth, Minnesota.
Parani, M., Lokhande, G., Singh, A., Gaharwar, A.K., 2016. Engineered nanomaterials for infection control and healing acute and chronic wounds. ACS Applied Materials & Interfaces 8, 10049-10069.
Paul, A., Eun, C.J., Song, J.M., 2014. Cytotoxicity mechanism of non-viral carriers polyethylenimine and poly-l-lysine using real time high-content cellular assay. Polymer 55, 5178-5188.
Rzhepishevska, O., Hakobyan, S., Ruhal, R., Gautrot, J., Barbero, D., Ramstedt, M., 2013. The surface charge of anti-bacterial coatings alters motility and biofilm architecture. Biomaterials Science 1, 589-602.
Santiago-Morales, J., Amariei, G., Leton, P., Rosal, R., 2016. Antimicrobial activity of poly(vinyl alcohol)-poly(acrylic acid) electrospun nanofibers. Colloids and Surfaces B: Biointerfaces 146, 144-151.
Shi, C., He, Y., Feng, X., Fu, D., 2015. ε-Polylysine and next-generation dendrigraft poly-L-lysine: chemistry, activity, and applications in biopharmaceuticals. Journal of Biomaterials Science, Polymer Edition 26, 1343-1356.
Shi, C., Zhao, X., Liu, Z., Meng, R., Chen, X., Guo, N., 2016. Antimicrobial, antioxidant, and antitumor activity of epsilon-poly-L-lysine and citral, alone or in combination. Food & Nutrition Research 60, 31891.
Simões, D., Miguel, S.P., Ribeiro, M.P., Coutinho, P., Mendonça, A.G., Correia, I.J., 2018. Recent advances on antimicrobial wound dressing: A review. European Journal of Pharmaceutics and Biopharmaceutics 127, 130-141.
Song, K., Wu, Q., Qi, Y., Kärki, T., 2017. Electrospun nanofibers with antimicrobial properties, in: Afshari, M. (Ed.), Electrospun Nanofibers. Woodhead Publishing, pp. 551-569.
Sood, A., Granick, M.S., Tomaselli, N.L., 2014. Wound dressings and comparative effectiveness data. Advances in Wound Care 3, 511-529.

Symonds, P., Murray, J.C., Hunter, A.C., Debska, G., Szewczyk, A., Moghimi, S.M., 2005. Low and high molecular weight poly(l-lysine)s/poly(l-lysine)–DNA complexes initiate mitochondrial-mediated apoptosis differently. FEBS Letters 579, 6191-6198.
Tavakoli, J., Mirzaei, S., Tang, Y., 2018. Cost-effective double-layer hydrogel composites for wound dressing applications. Polymers 10, 305.
Ushimaru, K., Hamano, Y., Katano, H., 2017. Antimicrobial activity of ε-poly-l-lysine after forming a water-insoluble complex with an anionic surfactant. Biomacromolecules 18, 1387-1392.
Wang, R., Zhou, B., Xu, D.-l., Xu, H., Liang, L., Feng, X.-h., Ouyang, P.-k., Chi, B., 2016. Antimicrobial and biocompatible ε-polylysine–γ-poly(glutamic acid)–based hydrogel system for wound healing. Journal of Bioactive and Compatible Polymers 31, 242-259.
Whittam, A.J., Maan, Z.N., Duscher, D., Wong, V.W., Barrera, J.A., Januszyk, M., Gurtner, G.C., 2016. Challenges and opportunities in drug delivery for wound healing. Advances in Wound Care 5, 79-88.
Ye, R., Xu, H., Wan, C., Peng, S., Wang, L., Xu, H., Aguilar, Z.P., Xiong, Y., Zeng, Z., Wei, H., 2013. Antibacterial activity and mechanism of action of □-poly-L-lysine. Biochemical and Biophysical Research Communications 439, 148-153.
Yoshida, T., Nagasawa, T., 2003. ε-Poly-L-lysine: microbial production, biodegradation and application potential. Applied Microbiology and Biotechnology 62, 21-26.
Zhou, C., Zhou, X., Su, X., 2017. Noncytotoxic polycaprolactone-polyethyleneglycol-ε-poly(l-lysine) triblock copolymer synthesized and self-assembled as an antibacterial drug carrier. RSC Advances 7, 39718-39725.
Zustiak, S.P., Wei, Y., Leach, J.B., 2013. Protein–hydrogel interactions in tissue engineering: Mechanisms and applications. Tissue Engineering Part B, Reviews 19, 160-171.

SUPPLEMENTARY MATERIAL

Biocompatible antimicrobial electrospun nanofibers functionalized with ε-poly-L-lysine

Georgiana Amariei[1], Vanja Kokol[2], Vera Vivod[2], Karina Boltes[1], Pedro Letón[1], Roberto Rosal[1,*]

[1] Department of Chemical Engineering, University of Alcalá, E-28871 Alcalá de Henares, Madrid, Spain
[2] Institute of Engineering Materials and Design, University of Maribor, SI-2000, Maribor, Slovenia

*Corresponding author: roberto.rosal@uah.es, Tel.: +34918856395, Fax: +34918855088

Contents

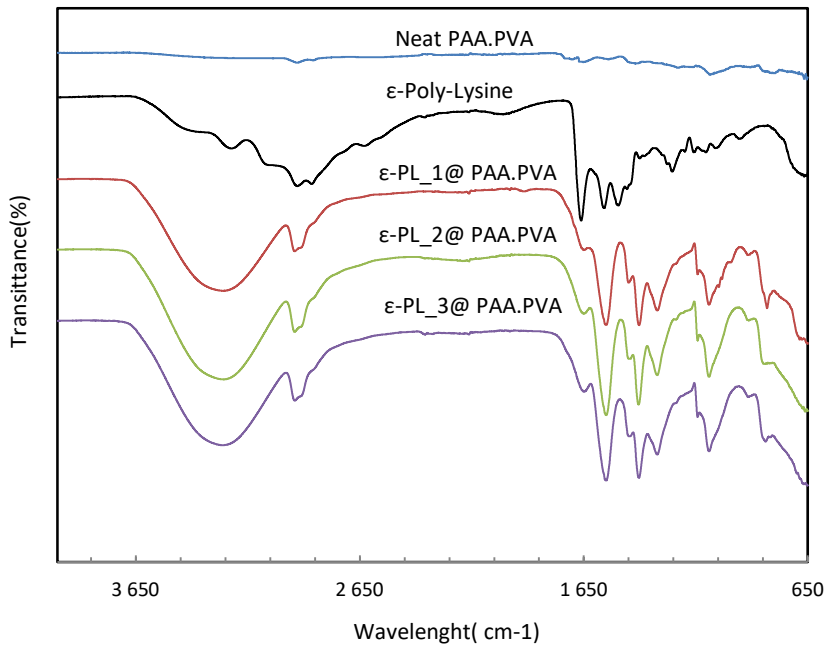

Figure S1. FTIR-ATR spectra of nanofibers functionalized at pH 10.

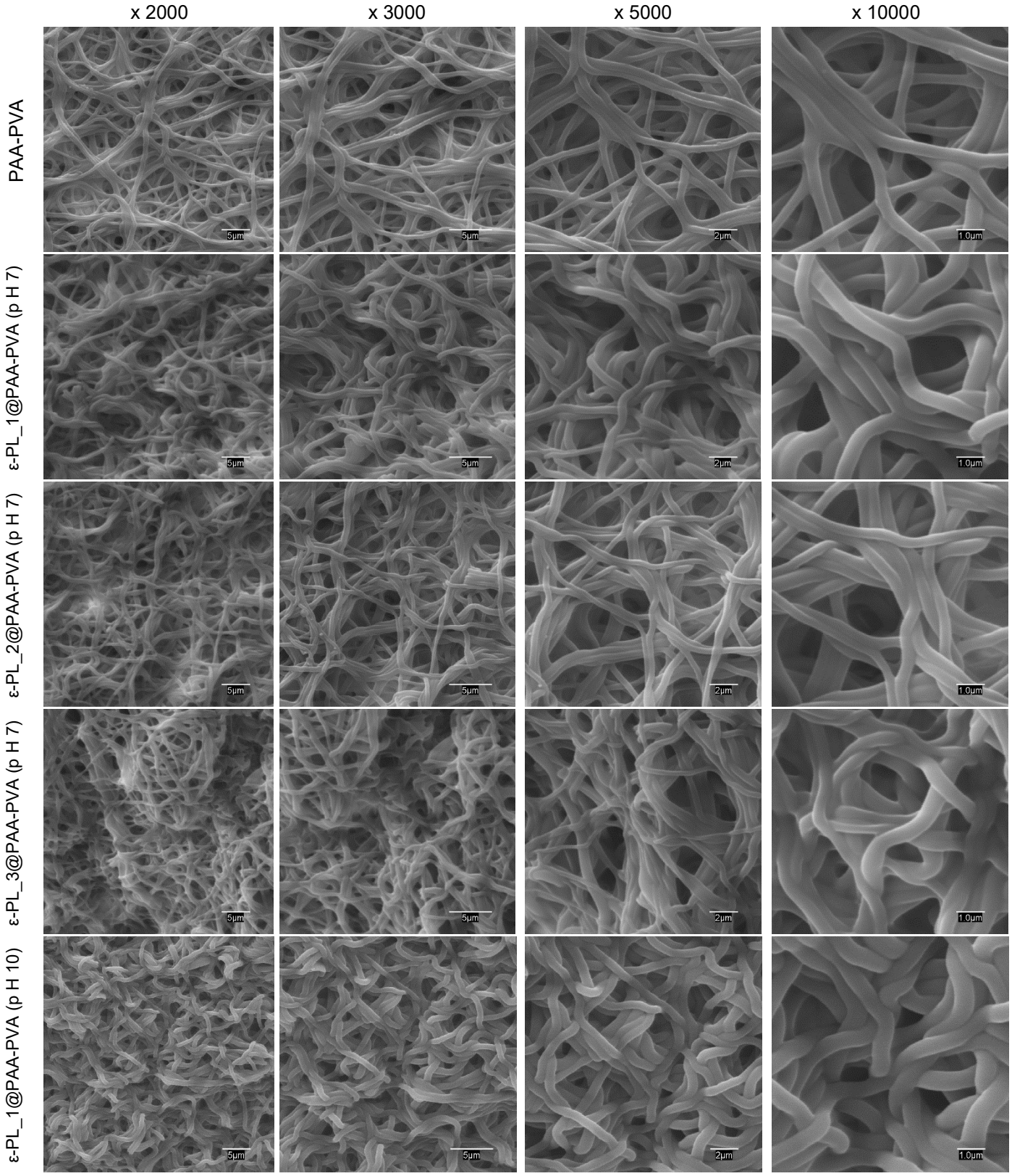
x 2000
x 3000
x 5000
x 10000
PAA-PVA
ε-PL_1@PAA-PVA (p H 7)
ε-PL_2@PAA-PVA (p H 7)
ε-PL_3@PAA-PVA (p H 7)
ε-PL_1@PAA-PVA (p H 10)
5µm
2µm
1.0µm

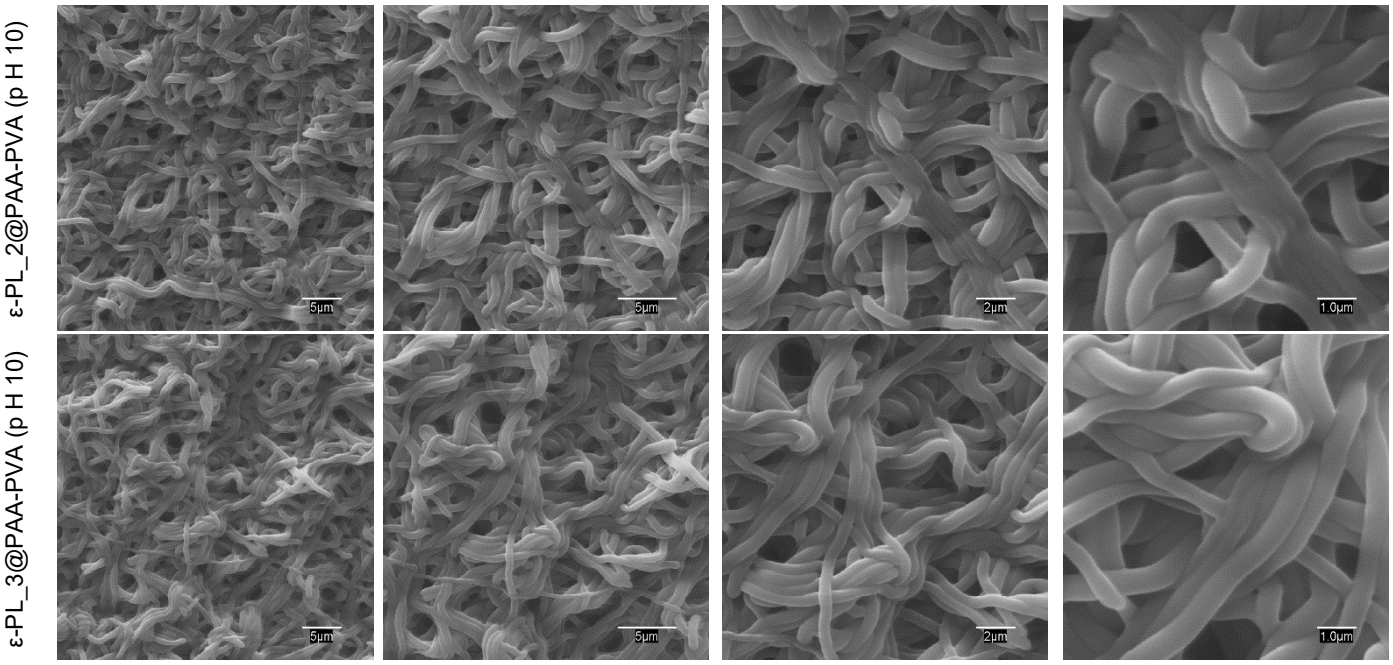

Figure S2. SEM images of nanofibers before impregnation (PAA-PVA), and nanofibers after impregnation with ε-Poly-Lysine (ε-PL) at pH 7 and 10.

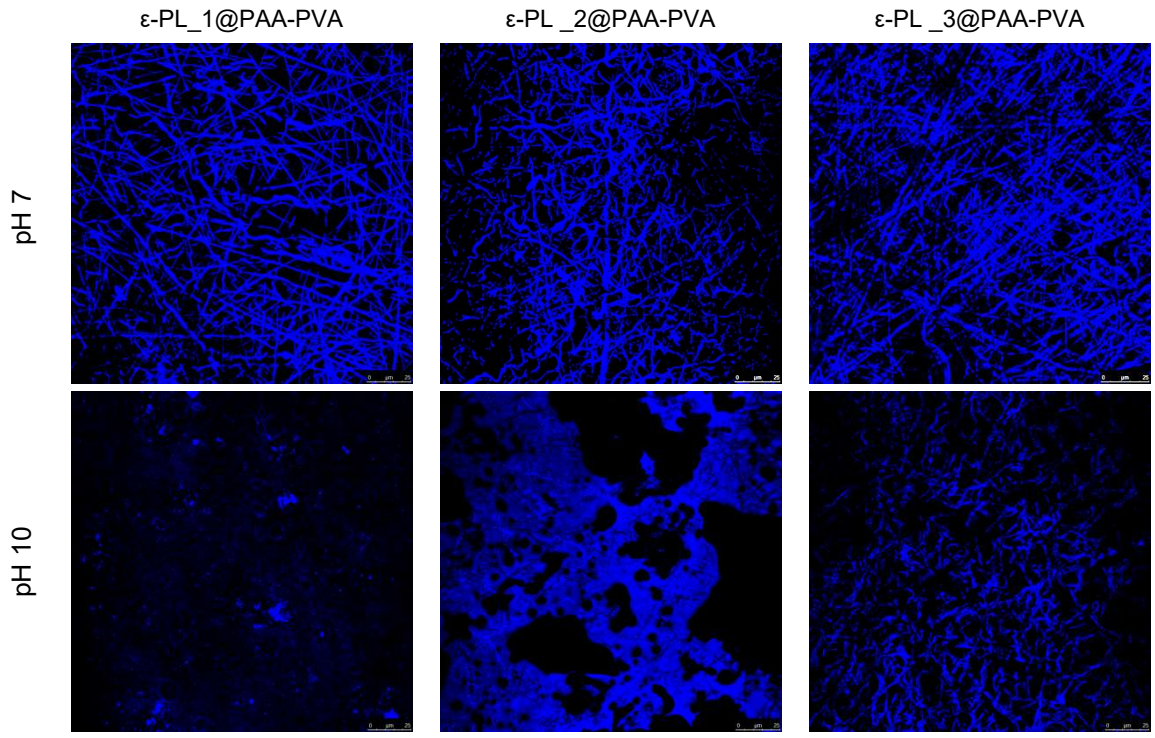

Figure S3. Confocal laser scanning microscopy images of ε-PL-loaded dressings after conjugation with fluorescamine.

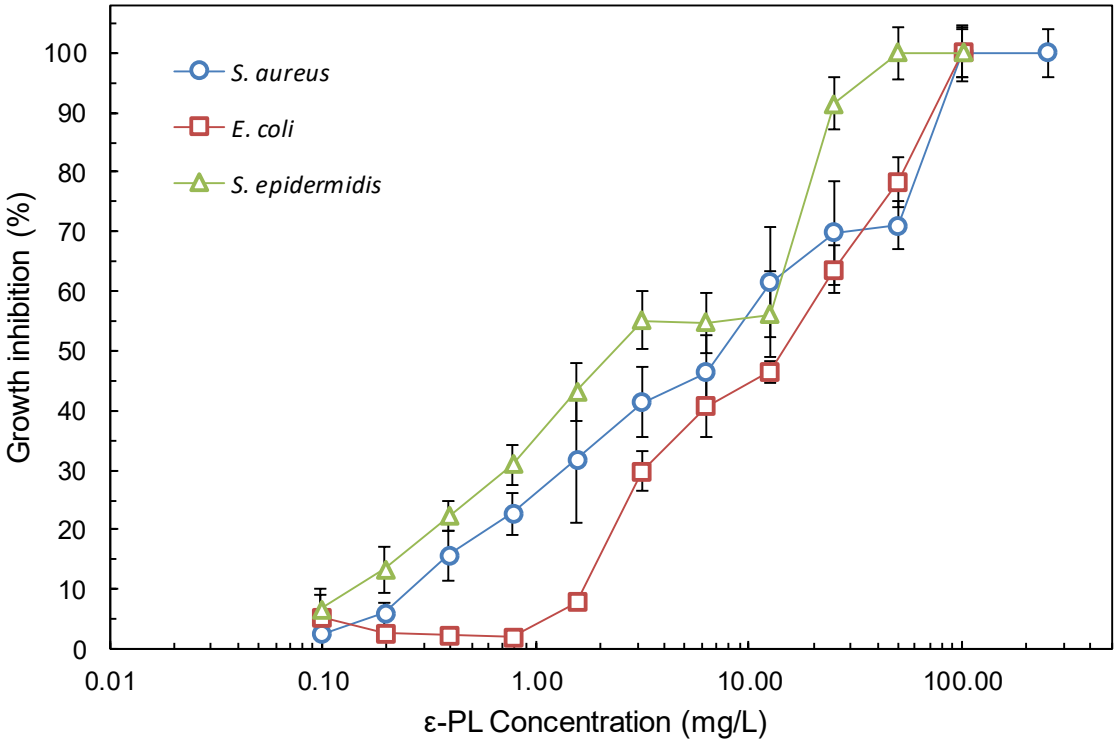

Figure S4. Growth inhibition measured from CFU counting after 20 h incubation at 37 °C as a function of ε-PL concentration.

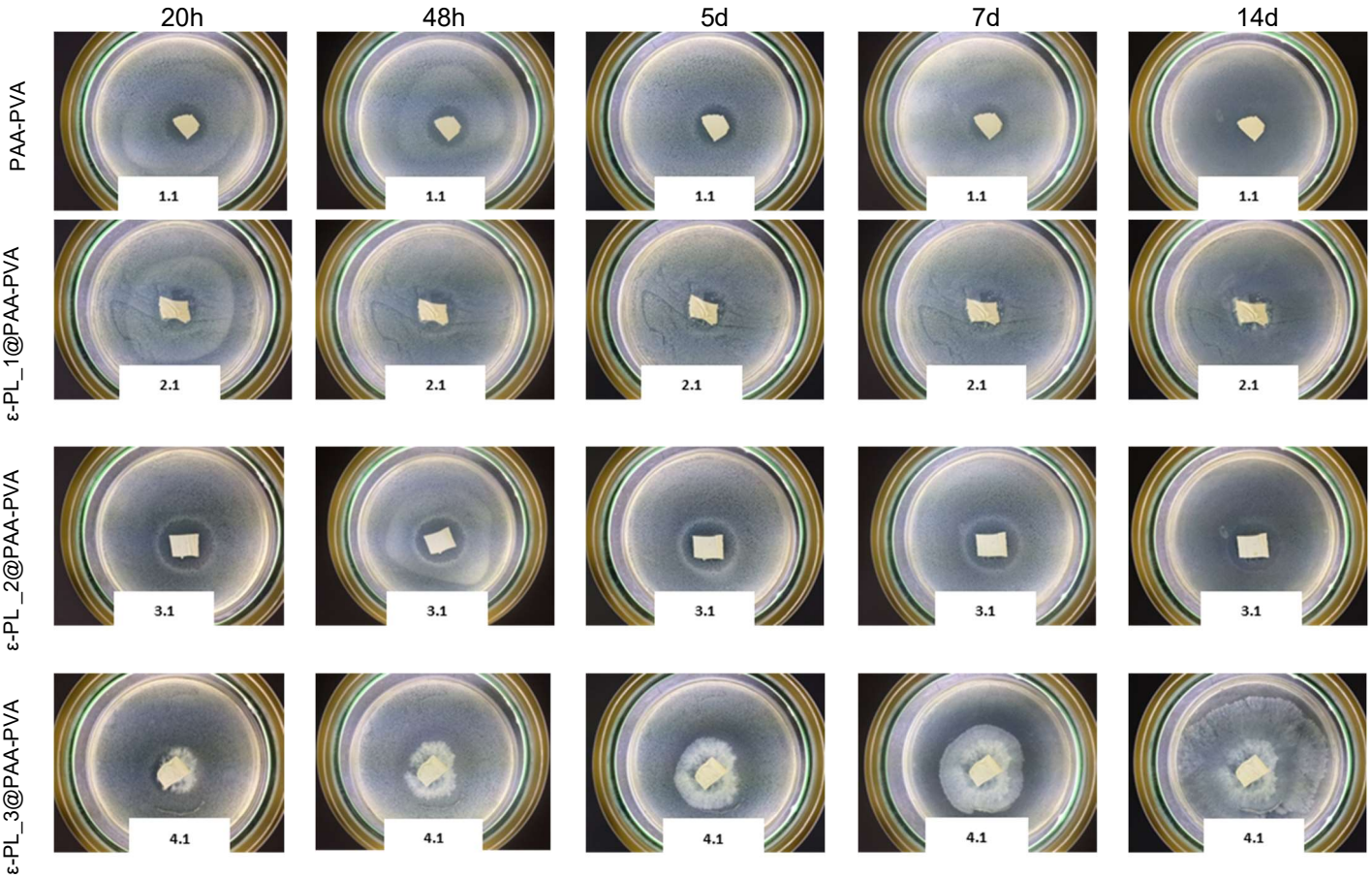

Figure S5. Halo inhibition zone experiments for the membranes prepared in this work (pH 7) along 14-day experiments in contact with *S. epidermidis* cultures in agar plates at 37 °C.

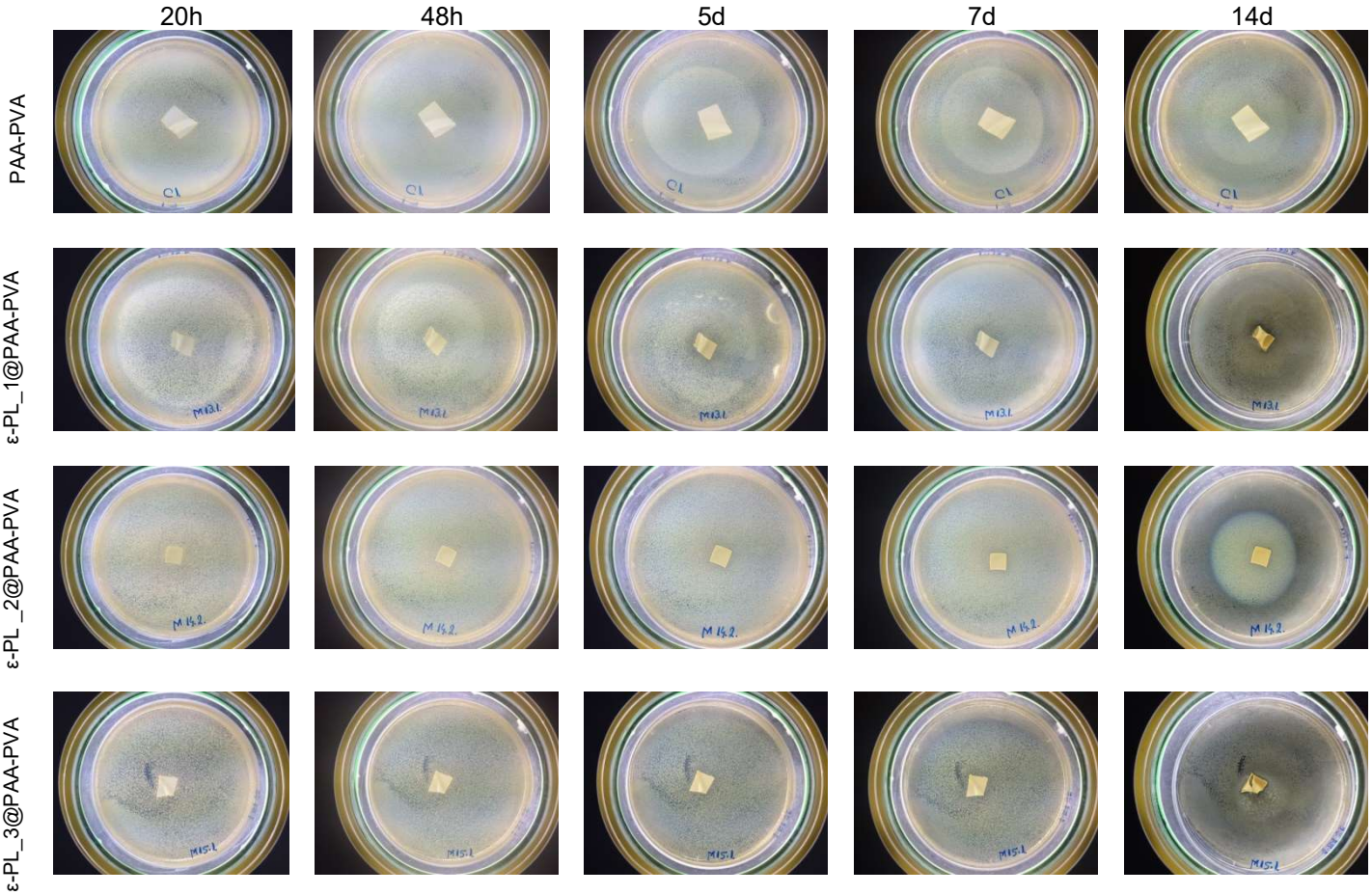

Figure S6. Halo inhibition zone experiments for the membranes prepared in this work (pH 7) along 14-day experiments in contact with *S. aureus* cultures in agar plates at 37 °C.

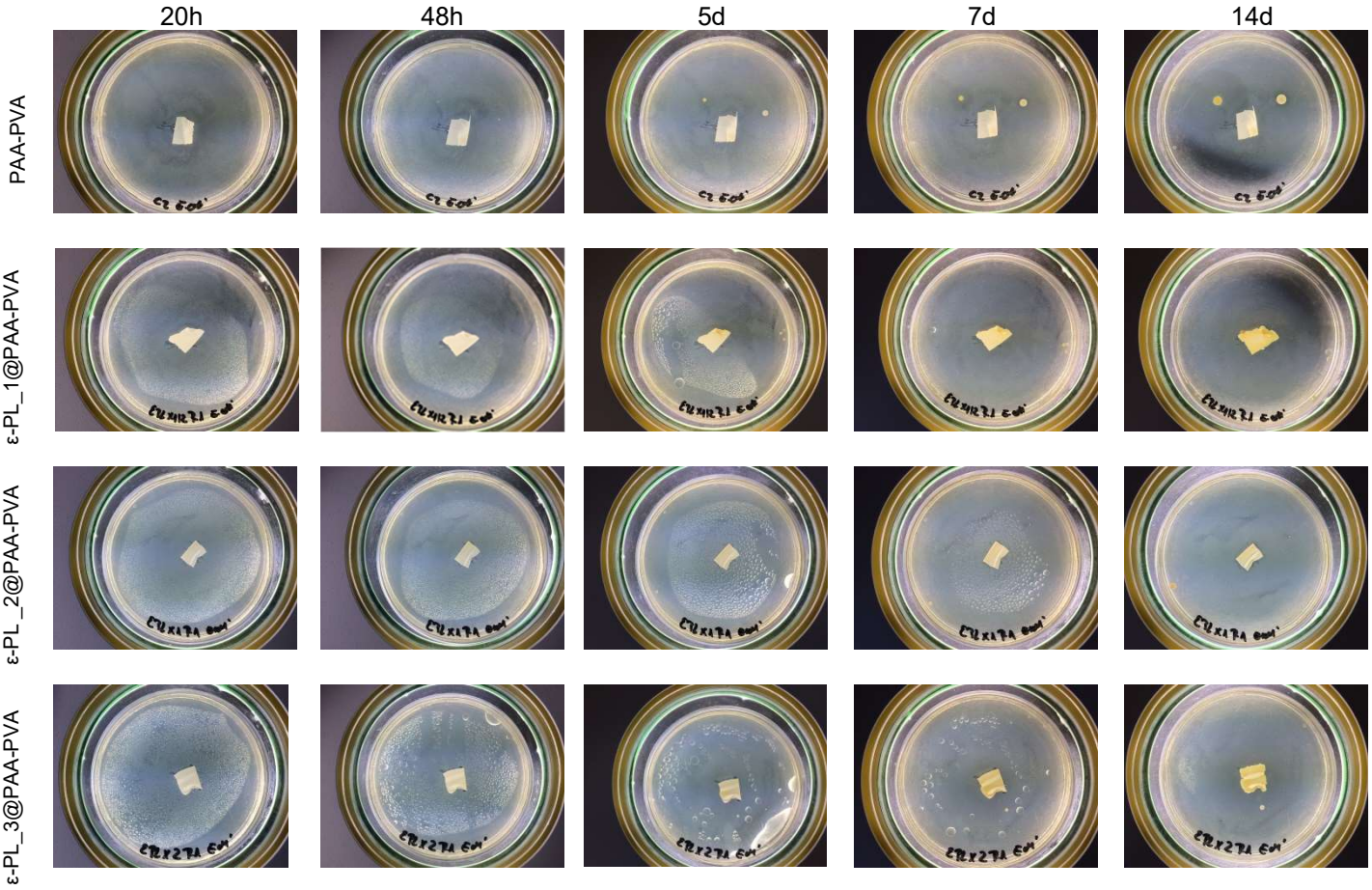

Figure S7. Halo inhibition zone experiments for the membranes prepared in this work (pH 7) along 14-day experiments in contact with *E. coli* cultures in agar plates at 37 °C.

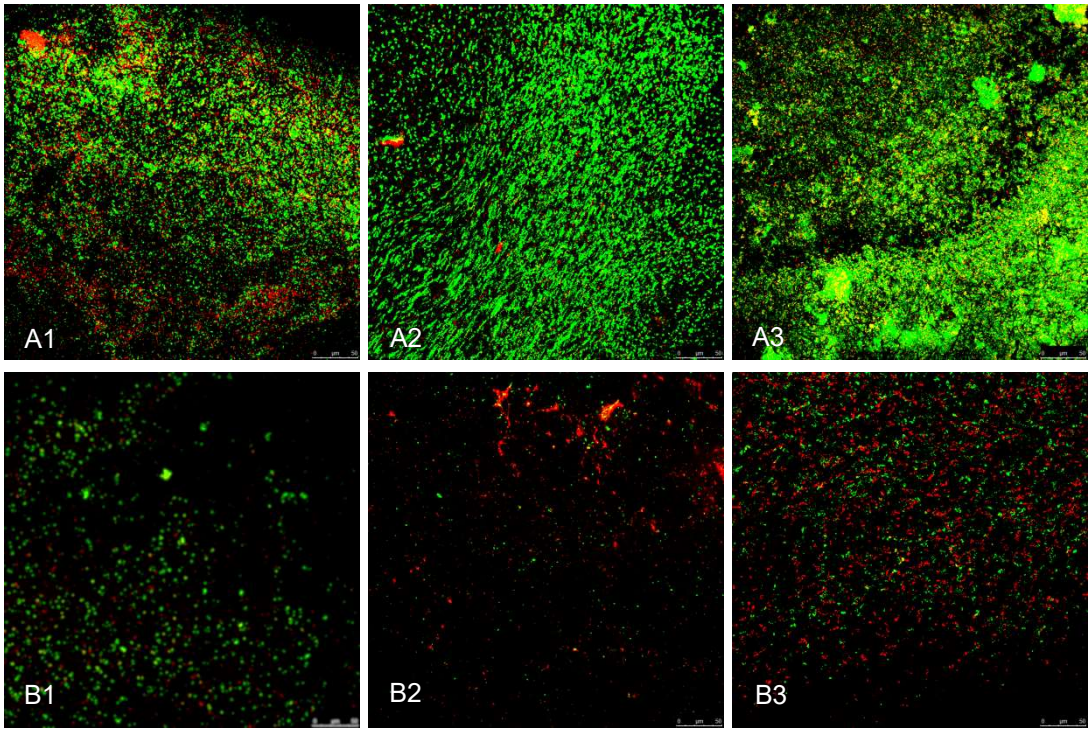

Figure S8. Live/Dead Confocal micrographs of PAA-PVA (A) and ε-PL_1@PAA-PVA (B) dressings after 14 days in contact with *S. aureus* (A1, B1), *S. epidermidis* (A2, B2) and *E. coli* (A3, B3) cultures at 37 °C.

A

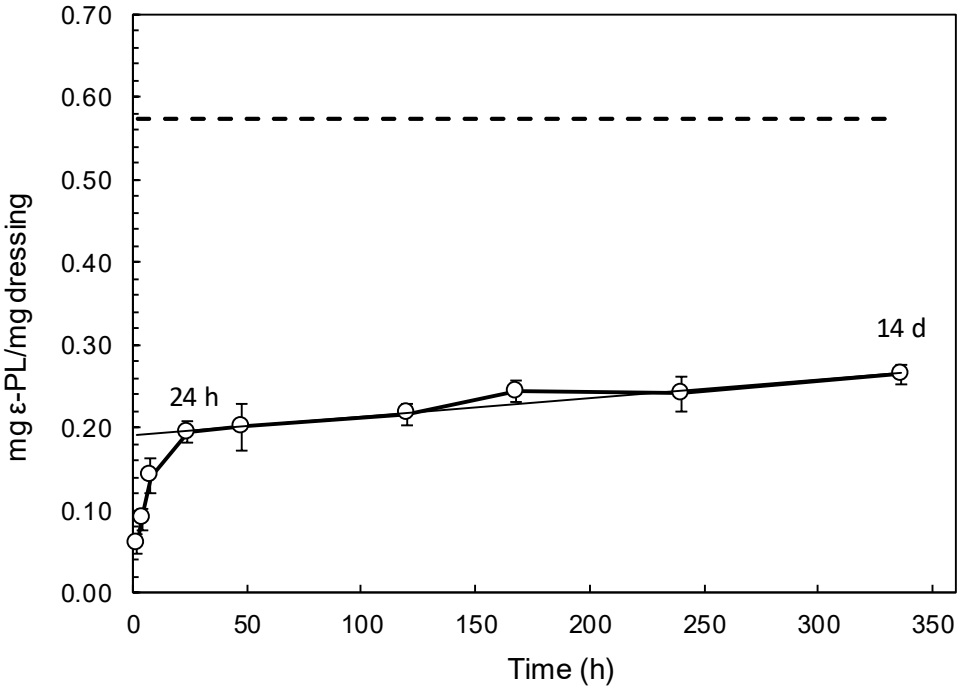

B

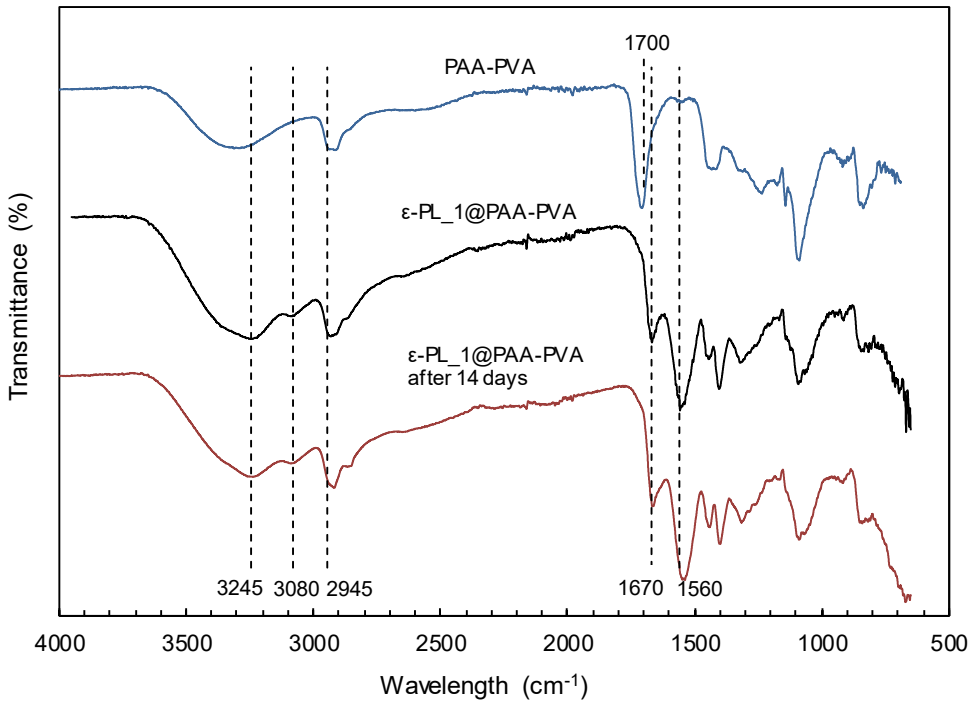

Figure S9. Cumulative release of ε-PL in PBS, pH 7.4 (A, the dashed line represents dressing loading); ATR-FTIR spectra of PAA-PVA and ε-PL_1@PAA-PVA dressings before and after 14 days at pH 7.4 (B).